LES of a Jet Excited by the Localized Arc Filament Plasma Actuators

Clifford A. Brown
Glenn Research Center, Cleveland, Ohio

NASA STI Program . . . in Profile

Since its founding, NASA has been dedicated to the advancement of aeronautics and space science. The NASA Scientific and Technical Information (STI) program plays a key part in helping NASA maintain this important role.

The NASA STI Program operates under the auspices of the Agency Chief Information Officer. It collects, organizes, provides for archiving, and disseminates NASA's STI. The NASA STI program provides access to the NASA Aeronautics and Space Database and its public interface, the NASA Technical Reports Server, thus providing one of the largest collections of aeronautical and space science STI in the world. Results are published in both non-NASA channels and by NASA in the NASA STI Report Series, which includes the following report types:

- TECHNICAL PUBLICATION. Reports of completed research or a major significant phase of research that present the results of NASA programs and include extensive data or theoretical analysis. Includes compilations of significant scientific and technical data and information deemed to be of continuing reference value. NASA counterpart of peer-reviewed formal professional papers but has less stringent limitations on manuscript length and extent of graphic presentations.

- TECHNICAL MEMORANDUM. Scientific and technical findings that are preliminary or of specialized interest, e.g., quick release reports, working papers, and bibliographies that contain minimal annotation. Does not contain extensive analysis.

- CONTRACTOR REPORT. Scientific and technical findings by NASA-sponsored contractors and grantees.

- CONFERENCE PUBLICATION. Collected papers from scientific and technical conferences, symposia, seminars, or other meetings sponsored or cosponsored by NASA.

- SPECIAL PUBLICATION. Scientific, technical, or historical information from NASA programs, projects, and missions, often concerned with subjects having substantial public interest.

- TECHNICAL TRANSLATION. English-language translations of foreign scientific and technical material pertinent to NASA's mission.

Specialized services also include creating custom thesauri, building customized databases, organizing and publishing research results.

For more information about the NASA STI program, see the following:

- Access the NASA STI program home page at *http://www.sti.nasa.gov*

- E-mail your question via the Internet to *help@sti.nasa.gov*

- Fax your question to the NASA STI Help Desk at 443–757–5803

- Telephone the NASA STI Help Desk at 443–757–5802

- Write to:
  NASA Center for AeroSpace Information (CASI)
  7115 Standard Drive
  Hanover, MD 21076–1320

LES of a Jet Excited by the Localized Arc Filament Plasma Actuators

Clifford A. Brown
Glenn Research Center, Cleveland, Ohio

National Aeronautics and
Space Administration

Glenn Research Center
Cleveland, Ohio 44135

April 2011

Acknowledgments

Level of Review: This material has been technically reviewed by technical management.

Available from

LES of a Jet Excited by the Localized Arc Filament Plasma Actuators

Clifford A. Brown
National Aeronautics and Space Administration
Glenn Research Center
Cleveland, Ohio 44135

Abstract

The fluid dynamics of a high-speed jet are governed by the instability waves that form in the free-shear boundary layer of the jet. Jet excitation manipulates the growth and saturation of particular instability waves to control the unsteady flow structures that characterize the energy cascade in the jet. The results may include jet noise mitigation or a reduction in the infrared signature of the jet. The Localized Arc Filament Plasma Actuators (LAFPA) have demonstrated the ability to excite a high-speed jets in laboratory experiments. Extending and optimizing this excitation technology, however, is a complex process that will require many tests and trials. Computational simulations can play an important role in understanding and optimizing this actuator technology for real-world applications. Previous research has focused on developing a suitable actuator model and coupling it with the appropriate computational fluid dynamics (CFD) methods using two-dimensional spatial flow approximations. This work is now extended to three-dimensions $(3-D)$ in space. The actuator model is adapted to a series of discrete actuators and a $3-D$ **LES** simulation of an excited jet is run. The results are used to study the fluid dynamics near the actuator and in the jet plume.

I. Introduction

The noise created by a supersonic aircraft is a primary concern in the development of future high-speed planes. The high thrust and low drag requirements of supersonic cruise limit the size engine, increasing jet exit velocity and resulting in high engine noise levels at takeoff and landing. The NASA Fundamental Aeronautics Program, Supersonics Project is tasked with developing fundamental technologies that make supersonic flight practical for regular travel. In order to meet this goal, engine noise must be reduced to a level that allows supersonic aircraft to enter and leave most airports without causing an excessive disturbance.

The naturally chaotic fluid dynamics in a high-speed jet plume are not easily controlled. The overwhelming energy of the jet and the lack of control surfaces downstream of the nozzle exit combine to resist control of the jet. Jets, however, have inherent preferred instabilities that, if appropriately perturbed, will grow as the plume develops and alter the downstream structure of the jet. Properly applied, jet excitation enhances a particular instability to change the downstream characteristics of the jet in a predictable way. Each application will excite a different combination of jet instabilities to achieve an end result and, therefore, it is important to understand the jet dynamics in order to optimize the excitation.

The free-shear boundary layer that forms between a high-speed jet flow and the surrounding fluid is naturally unstable. As the jet mixes with its surroundings, Kelvin-Helmholtz instability waves are formed in the boundary region. These instability waves grow and decay as the jet develops, governing the formation and destruction of the unsteady turbulent flow structures that characterize the energy cascade in the jet. By targeting particular instability waves, jet excitation can alter the flow structures that are responsible for the transport of mass and the transport and dissipation of energy in the jet plume. Moreover, a large change in the jet dynamics can be achieved with a minimal excitation energy if the excitation is input at the nozzle exit where the instability waves, and therefore the flow structures, are small and less energetic. It is this ability to make large changes in the jet with relatively little energy that gives jet excitation so much potential.

Jet excitation must exploit the natural instabilities in the jet to exert control over the on the turbulent structures in the jet plume or the energy of the jet will overwhelm the input perturbation. Proper excitation

requires intelligently selecting the best combination of instabilities from the infinite number of possibilities to maximize the desired effect. Modern experimental techniques, such as particle image velocimetry and phased array microphones, can provide detailed flow and noise data that may be used to optimize the excitation but these experiments are often too costly for the large number of cases required for a true optimization, especially at a larger and more realistic test facility. Numerical simulations can provide a cost effective alternative to experiments for optimizing the excitation.

Numerical simulations of excited jets are large computations. Typically, these simulations include all or part of the nozzle, the flow actuators, and the jet plume. Therefore, the length- and time-scales in an excited jet simulation range from the smallest flow structures in the nozzle boundary layer to the large-scale flow structures in the jet plume forcing a large domain with a relatively small time step. Previous research has investigated the excited jet problem using several computation scheme and, although these simulations were simplified using either an axisymmetric or two dimension $(2 - D)$ assumption in space (depending on the scheme), determined that a Large Eddy Simulation (LES) was needed to capture the unsteady fluid dynamics in the plume of the excited jet.[1] Using the knowledge gained in these simulations, the LES computations are extended to three dimensions $(3 - D)$. The knowledge gained in this first $3 - D$ simulation will be used in future simulations that will optimize the jet excitation for noise reduction or study the scalability of the excited jet and flow actuator system for deployment on an aircraft engine.

Jet excitation, properly applied, has the potential to reduce aircraft engine noise at takeoff and landing while not affecting the cruise performance of the aircraft. Furthermore, developments in flow actuator technology, such as the Localized Arc Filament Plasma Actuator (LAFPA) developed at Ohio State University (OSU) Gas Dynamics and Turbulence Laboratory, offer hope that excitation could be deployed on larger jets in more realistic situations if the noise benefit is proven. Current research to demonstrate the noise reduction potential of jet excitation and to adapt the flow actuators to larger more realistic jets is ongoing under the Airport Noise section of the Supersonics Project and developing accurate simulations of an excited jet is an important part of this effort.

II.   Computational Methodology

II.A.   LAFPA Model

The Localized Arc Filament Plasma Actuators (LAFPA) have been developed as a high amplitude, high frequency flow actuator at Ohio State University (OSU). These actuators have demonstrated the ability to excite a small-scale $(D_j = 1.0\,in.)$ high-speed jet[2] and, to a lesser extent, a larger $(D_j = 7.5\,in.)$ high Reynolds number jet.[3] The LAFPA use high voltage electronics to create small regions of plasma by periodically and rapidly heating the air in a small cavity near the nozzle exit. Although there are three forces typically associated with plasma dynamics (electrohydrodynamic, magnetohydrodynamic, and Joule heating), research as indicated that the Joule heating is the primary forcing mechanism in the high-speed flow environment of a jet.[4] The rapid Joule heating ejects the hot gas from the cavity while creating a shock wave that travels away from the actuator cavity and impacts the jet.[5–7] A computational model of the LAFPA, therefore, must simulate the rapid heating of the plasma actuator in a way that allows the simulation to generate the associated shock wave and eject the hot gas from the actuator cavity.

There are a few factors to consider when developing a model of the LAFPA for use in a CFD simulation in addition to capturing the actuator physics. First, the short time-scale and sharp flow gradients of the actuator may make the simulation numerically unstable. As a result, additional grid density may be required near the actuator and the maximum stable time step of simulation reduced, increasing the computation time needed by the simulation. Second, the actuator model should be applicable to a wide range of commercial and development CFD codes. Finally, the model should minimize the amount of time expended by the user. Preliminary research, used 2-D simulations, has been conduced using two different actuator models. The first one adds periodic source terms to the governing flow equations that simulate the actuators.[5] The second model adds the actuator energy to the initial flow condition and allows the CFD solver to compute the effect of this energy using the standard flow equations.[1,8] Each model has advantages and disadvantages. The source terms, for example, require minimal user intervention and can include the effect of a short temperature rise time. However, not all CFD codes include (or allow the user to access) source terms where almost all codes allow the user to set the flow initial condition. While this is an advantage of the initial condition model, it does not include any actuator time component and requires the user to reset the initial flow condition at the beginning of each actuator cycle. Ultimately, the initial condition model was selected for the 3-D simulations because of the portability between CFD codes it affords.

A model of the LAFPA must simulate the rapid Joule heating, and initialize the resulting pressure waves, at the proper circumferential locations near the nozzle exit. There are two significant assumptions inherent to an actuator model based on the initial flow condition. First, the experimental LAFPA hardware does not instantly reach its maximum temperature. Rather, emission spectroscopy measurements conducted at OSU indicate that the temperature rises over a period of $10 - 20\,\mu s$.[4] The initial condition model assumes that all temperature change occurs during a period of less than one time step (unresolved by the CFD solver). Previous experience, however, indicates that the maximum stable time step will be significantly less than $10\,\mu s$.[1,8] The LAFPA model, therefore, assumes that the temperature rise time is not critical to the downstream flow dynamics. Second, the LAFPA used in the experiments do not turn off instantly but are programed to remain on for some percentage of the forcing period (the actuator duty cycle). As an energy pulse that is unresolved by the CFD solver, the LAFPA model assumes that the primary forcing mechanism is the initial breakdown of air into plasma, and the shock wave it generates. Thus, the affect of the duty cycle is assumed to be negligible. These are the two assumptions required by the initial condition model that must be validated by comparing the simulation results against experimental data downstream in the jet plume.

The initial condition LAFPA model is implemented by periodically stopping the CFD solver and resetting the internal energy in the desired locations to form a new initial flow condition that reflects the addition of the actuator energy. Specifically, the actuator model is implemented in several steps. First, the actuator temperature (T_A), determined from experimental measurements (i.e. emission spectroscopy) or as the result of a calibration procedure. At this point careful attention should be given to correctly non-dimensionalize each variable based on the conventions followed in the CFD solver that will be used for the simulation. The actuator temperature is then used to the calculate the pressure associated with the actuator (P_A) using the ideal gas law. Note that use of the ideal gas law is an additional assumption in the model but is not inherent to the model itself. This relationship may change based on data collected from experiments and simulations. Next the actuator pressure is used to compute the peak actuator energy ($E_{A,peak}$) as:

$$E_{A,peak} = \frac{P_A}{\rho(\gamma - 1)} \tag{1}$$

A Gaussian shape factor is then applied to the peak actuator energy to eliminate any discontinuities in the initial condition data giving the final form of the actuator energy (E_A) pulse as:

$$E_A = E_{A,peak}e^{-log(2)(xx+yy+\theta\theta)} \tag{2}$$

where:

$$xx = \frac{(x - x_0)^2}{x_w}, yy = \frac{(y - y_0)^2}{y_w}, \theta\theta = \frac{(\theta - \theta_n)^2}{\theta_w} \tag{3}$$

where the actuator center is (x_0, y_0, θ_n) with $\theta_n = 2\pi n/n_{actuators}$ for $n = 0, 1, ..., (n_{actuators} - 1)$ and x_w, y_w, and θ_w define the width of the actuator pulse in the axial, radial, and circumferential directions respectively. Finally, the actuator energy is added to (rather than replaces) the existing flow energy to create the new initial flow condition, allowing energy to build to an equilibrium in the cavity during the first few cycles if the actuator energy is not completely evacuated from the cavity during the current cycle (as might happen with a high frequency excitation).

The instability waves in a jet are characterized for excitation by an azimuthal mode and frequency. The azimuthal mode determines the phase difference between the actuators and the frequency, which is usually given as a non-dimensional Strouhal number ($St_{DF} = fD_j/U_j$), determines the actuator period. The number of time steps per actuator cycle may be calculated from the time step and the desired excitation Strouhal number. Note that each cycle may require multiple restarts to input the correct actuator phasing depending on the instability mode targeted for excitation. Simulations are run through several cycles to allow the actuators perturbations sufficient time to travel downstream and generate the jet response before acquiring any flow data.

II.B.   LES Solver - BASS

The Broadband Aeroacoustic Stator Simulation (BASS) code is currently being developed at the NASA Glenn Research Center as a general purpose CAA/LES flow solver for compressible flow simulations.[9,10]

The code solves the non-linear Euler or Navier-Stokes equations on generalized curvilinear grids using the chain rule form of the governing equations. BASS combines high-order spatial differencing methods with optimized explicit time marching schemes to accurately compute the unsteady flow dynamics. A shock-capturing artificial dissipation scheme with 10th order background dissipation is used to remove unresolved waves from the flow solution.[11] BASS has been used extensively on the prediction of tone and broadband noise from aircraft engine stators using the inviscid Euler equations[12,13] and is being developed to simulate the jet exhaust plume using the complete Navier-Stokes equations.

The BASS code employs and Implicit LES (ILES) strategy,[14] in which a 10th order artificial dissipation model is used to filter the sub-grid scale turbulence. The HALE-RK67 explicit time marching scheme[15] is used with the optimized fourth-order Dispersion Relation Preserving (DRP) spatial differencing scheme from Tam and Webb.[16] The Thompson boundary conditions are applied at the outer edges of the computational domain.[17,18] Sponge layers are also used near the Thompson boundaries to prevent spurious reflections from reentering the domain.[19]

A 3-D LES simulation of a jet requires significant computational resources and the plasma actuators only increase the computation time required. The LAFPA imposes severe gradients on the flow in the actuator region near the nozzle wall. The standard seven point stencil DRP one-sided difference scheme used to compute spatial derivatives at the boundaries was originally developed for simulations of inviscid flows and, indeed, this scheme works very well with flows in this regime. However, the standard seven point stencil may become numerically unstable for high wave number perturbations in wall bounded viscous flows when using the expected viscous time step.[20] The result is a significant reduction in the global time step enforced to maintain numerical stability at the viscous wall boundary inside of the nozzle and near the actuator.

The BASS code has been extensively developed for inviscid flow problems (i.e. rotor-stator interaction noise) and, therefore, defaults to the standard seven point stencil DRP one-sided difference scheme at the wall boundaries. These boundary stencils where replaced for the excited jet problem with the appropriate seven point MacCormack one-sided differencing stencil.[21] As implemented, the MacCormack based boundary stencil retains the dispersion characteristics of the $4^{th}-order$ DRP scheme used in the field, so that waves continue to propagate at the correct speed near the wall boundaries, while the dissipation increases to damp instabilities at the points nearest the wall. This combination of features is achieved by optimizing the coefficients to retain the dispersion performance while reducing the overall order of accuracy, to a $2^{nd}-order$ scheme, to increase the numerical dissipation. Note that this scheme is directional so that waves approaching the wall are dissipated while reflected waves are similarly amplified. Also, the overall order of accuracy of the simulation, based on a strict analysis of the numerical scheme, is reduced from $4^{th}-order$ to $2^{nd}-order$ (the order of accuracy at the boundaries). In practice, however, the grid spacing is sufficiently small in the near wall boundary region that the actual numerical error incurred by reducing the order of accuracy near the wall boundaries should be small compared to other parts of the computational domain where the grid spacing is much larger. Ultimately, the value of these MacCormack based stencils will be determined by the real increase in time step and the accuracy of the simulated flow data downstream in the jet plume.

II.C. Computational Grid

The geometry used in these simulations is based on the physical dimensions of a convergent nozzle with an exit diameter (D_j) of $1.0\,in.$ (figure 1) previously tested at Ohio State University.[2,3] A ceramic extension, measuring $0.5\,in.$ in the axial direction and $1.0\,in.$ in the radial direction, is attached to the nozzle to hold the actuators. With this extension in place, the nozzle features a straight section of $0.901\,in.$ from the final contraction to the nozzle exit and a nozzle lip thickness that is the same dimension as the nozzle diameter. The extension includes the actuator cavity which measures $0.059\,in.$ in the axial direction and $0.051\,in.$ in the radial direction. The cavity extends around the entire circumference of jet (spatial constants in the LAFPA model are used to set the arc length of the actuator at $0.118\,in.$ to match the electrode separation used in the experiments). These dimensions are replicated in the computational simulations.

The computational mesh was designed to capture the necessary unsteady fluid dynamics while minimizing the computational time required and maximizing the numerical stability of the solution in the actuator region. This balance was partially achieved by limiting the overall size of the domain and adding grid density in the actuator region. The domain (figure 2) was limited in the downstream direction to only $x/D_j = 10$. The radial boundary was sloped at a $7°$ angle, intersecting the nozzle exit plane $(x/D_j = 0)$ at $r/D_j = 8$, to enhance the numerical stability of the boundary condition by allowing a consistent inflow when a low-speed constant freestream flow is specified. Although this domain is small, the primary regions of interest in the

first $3-D$ trial case is near the actautor and in the initial jet shear layer where the actuator perturbations are expected to grow and peak (approximately $3D_j$ based on experimental data). The nozzle inflow boundary was placed in the straight section of the nozzle and upstream of the actuator cavity thus eliminating the nozzle contraction from the simulation. Although ideally the nozzle contraction should be included in the computation so that the wall boundary layer is correctly formed, the number of additional grid points required to resolve the boundary layer through the nozzle contraction significantly slowed the computation. In this case, the presence of a relatively long straight section after the contraction in the physical nozzle allows the contraction to be removed from the simulation while retaining the actual geometry of the experimental hardware near the nozzle exit. Sponge layers extend from the computational domain at the upstream, downstream, and radial boundaries in an effort to prevent spurious reflections caused by the boundary conditions from traveling back into the domain. These sponge layers are particularly important in these simulations given the proximity of the boundaries to the region of interest in the computational domain.

The grid topology was dictated, in large part, by the geometry of the actuator cavity. Although the dimensions of the cavity in the simulation where identical to the dimensions of the physical hardware, the corners of the cavity and at the nozzle lip were rounded, using small radius curves, rather than sharp. This was done to compensate for limitations in the viscous wall boundary scheme used in the BASS code. At that time, BASS had be primarily been developed for inviscid rotor-stator interaction simulations and, as a result, work on viscous flows was only beginning and BASS now includes the ability to handle sharp corner geometries. Nevertheless, the tight radius corners of the actuator cavity in close proximity to the nozzle exit used in this simulation made it difficult to form smooth grid lines while maintaining the grid density necessary. Figure 3 shows a streamwise and cross-stream slice of the grid topology at the actuator cavity. The GridPro/az3000 grid generation package from Program Development Corporation[22] was used to build the grid. Internal surfaces were placed around the cavity and nozzle exit to force grid points into the cavity and hold the grid density in the this region. The BASS code requires full face block matching throughout the grid so the remainder of the grid was built out from the block boundaries established at these internal surfaces.

Three-dimensional grids for round nozzles are commonly formed by simply extruding points from a $2-D$ layout in the azimuthal direction. While this is a relatively easy way to form a $3-D$ grid, it results in a singular axis at the jet centerline where the cell size and, therefore the maximum time step, approaches zero. Two-dimensional simulations have indicated that the energy pulse from the plasma actuator may actually penetrate the jet column to the centerline. If this occurs in the $3-D$ simulations, the discrete pulses from several actuators would combine at or near the nozzle centerline. So although CFD solvers generally have approximations built in to deal with a singular axis, it is better in this case to directly compute the centerline region. The grid topology was formed to include a transition from a polar grid near the nozzle to a Cartesian grid around the jet centerline (using 128 points in the azimuthal direction throughout the grid). This topology, shown in figure 3(b), allows the polar grid to smoothly wrap around the nozzle surfaces, which would be difficult to achieve with a Cartesian grid, while also allowing the flow flow to be directly calculated around the nozzle centerline without adjusting the CFD scheme and without the time step reduction that would be incurred with a complete polar grid.

The final grid was relatively small with approximately 12.5 million grid points. This reflects the small computation domain and rapid grid stretching, particularly in the axial direction, away from the nozzle. The rate of stretching was based roughly on the results from previous $2-D$ simulations.[1] Grid points were packed up to within $0.00025\,in.$ of the nozzle walls. It is important to note that this grid represents the first attempt to perform an unsteady $3-D$ simulation of an excited jet with the LAFPA and is, therefore, only a starting point. The results of this simulation will be used to examine adequacy of these grid parameters and provide direction for future simulations. A grid sensitivity study will be needed in this next stage of development.

III. Flow Results

III.A. Actuator Dynamics

A model of the Localized Arc Filament Plasma Actuators (LAFPA) has been developed for CFD simulations. The LAFPA model was applied to a 3-D LES simulation of a $M_j = 0.9$ isothermal jet. The actuator geometry, which was based on the arrangement used in prior experiments conducted at OSU,[2,3] included a total of 8 actuators evenly spaced around the circumference of the jet. The actuator temperature was assumed to
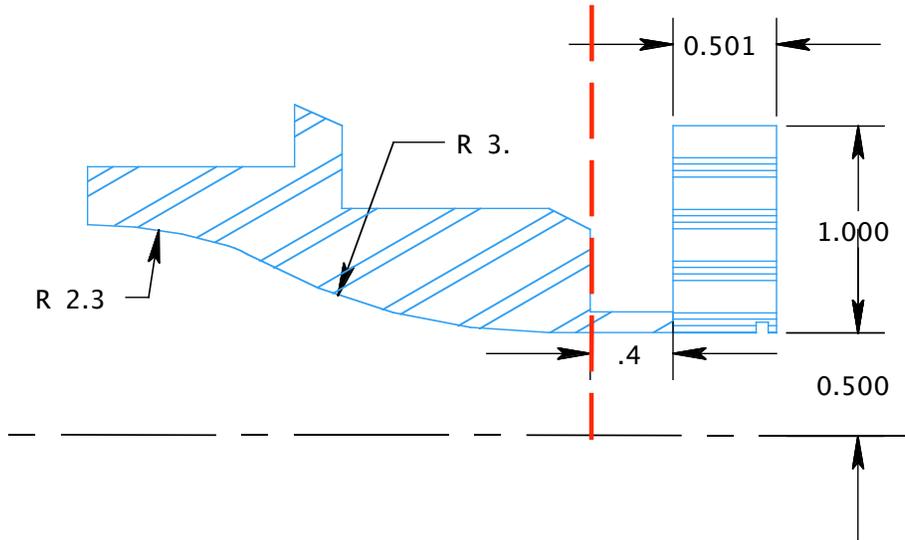
Figure 1. Schematic drawing of the nozzle used in the simulations. Note that only the area to the right of the vertical dashed line was included in the simulations.
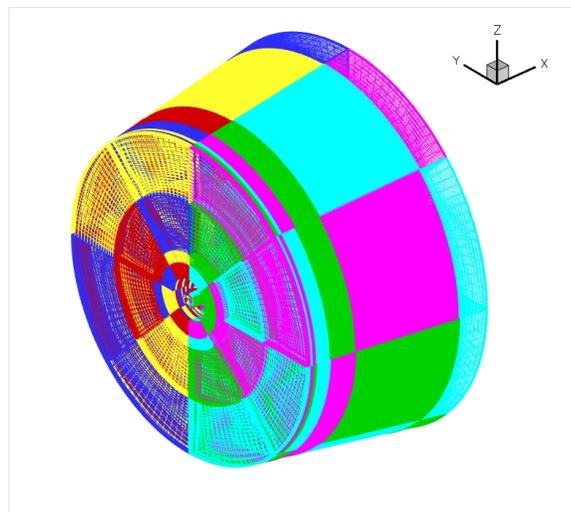

Figure 2. Computational mesh used for the excited jet simulations.

(a) Streamwise at $\theta = 0°$

(b) Cross-stream at $x = -0.06in.$
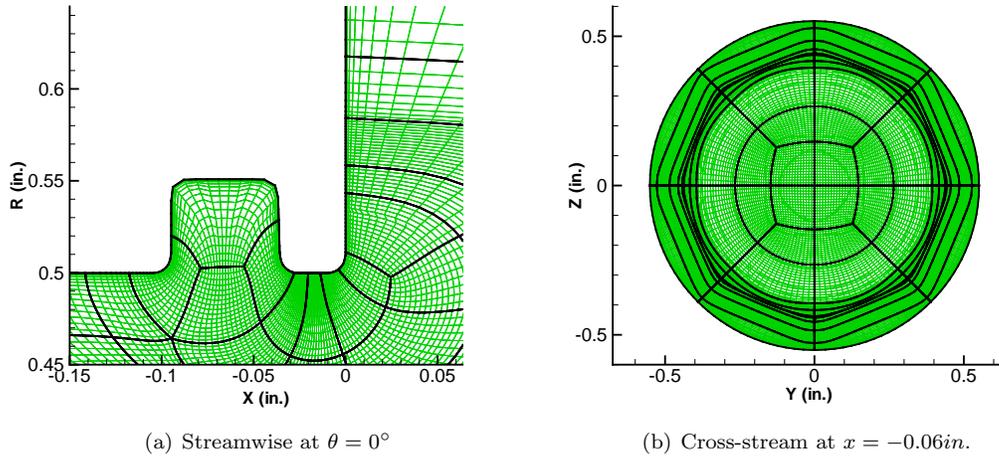
Figure 3. Cross-stream and streamwise views showing the grid topology around the actuator cavity.
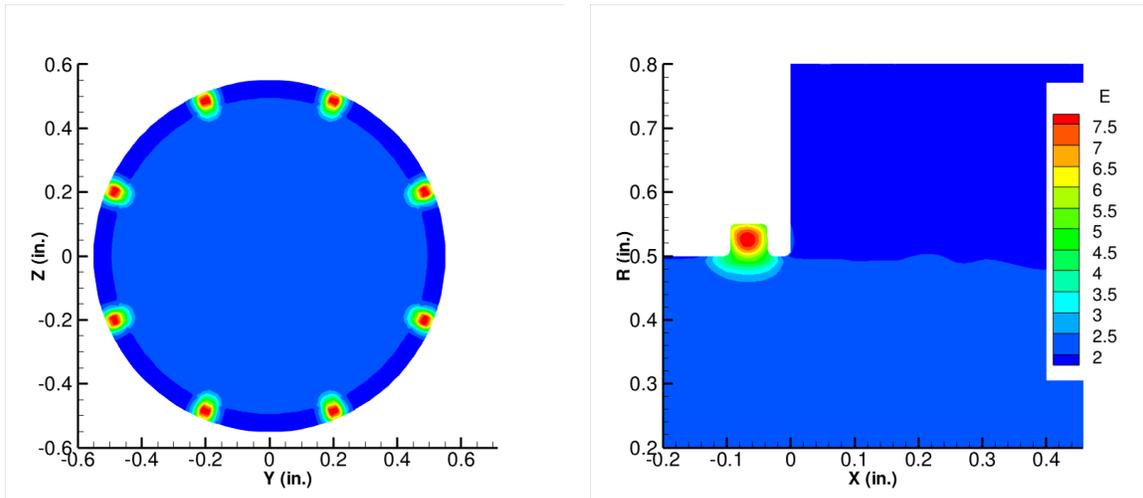

Figure 4. Cross-stream and streamwise view of the initial flow condition (non-dimensional internal energy) with the actuator present. Note that the energy contours in the baseline flow have been lost on this scale due to high amount of energy in the actuator.
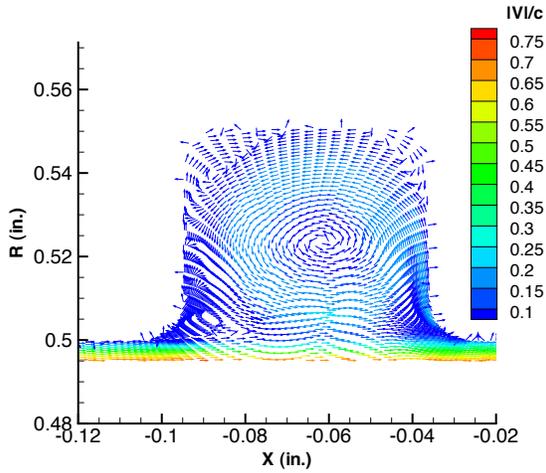
(a) $t = 0\,\mu s$
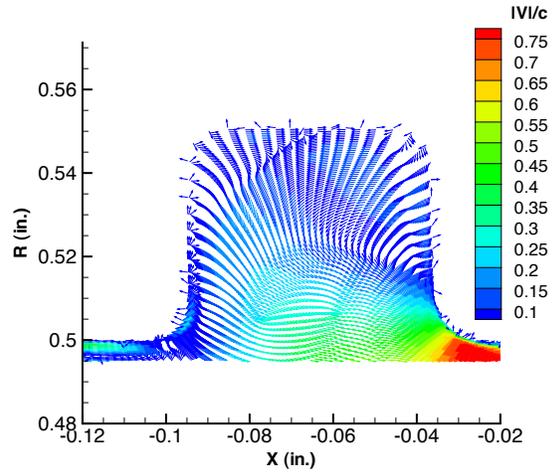
(b) $t = 5\,\mu s$
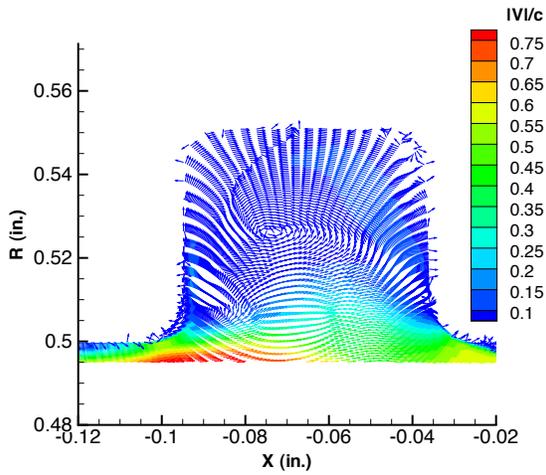
(c) $t = 10\,\mu s$
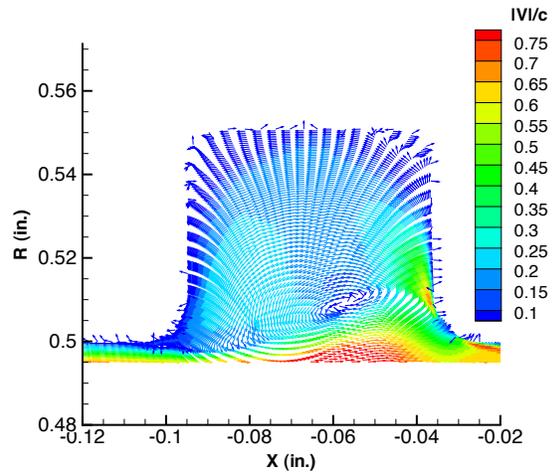
(d) $t = 15\,\mu s$
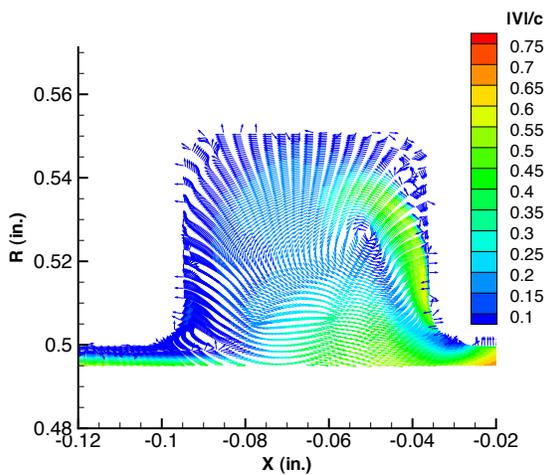
(e) $t = 20\,\mu s$
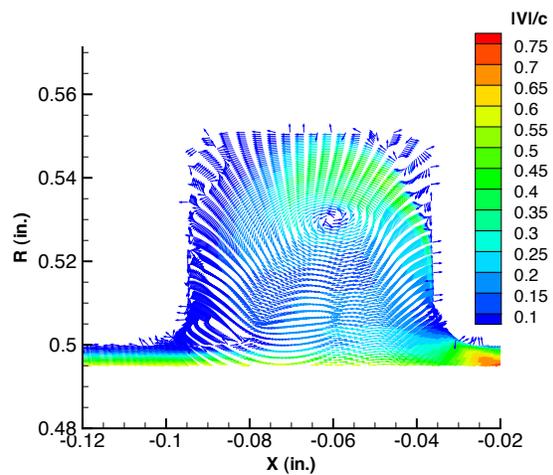
(f) $t = 25\,\mu s$

Figure 5. Velocity vectors near the actuator cavity at the beginning of a cycle.

(a) $t = 5\,\mu s, x = -0.06\,in.$

(b) $t = 5\,\mu s, \theta = 22.5°$

(c) $t = 10\,\mu s, x = -0.06$

(d) $t = 10\,\mu s, \theta = 22.5°$

(e) $t = 15\,\mu s, x = -0.06$

(f) $t = 15\,\mu s, \theta = 22.5°$

(g) $t = 20\,\mu s, x = -0.06$

(h) $t = 20\,\mu s, \theta = 22.5°$

(i) $t = 25\,\mu s, x = -0.06$

(j) $t = 25\,\mu s, \theta = 22.5°$
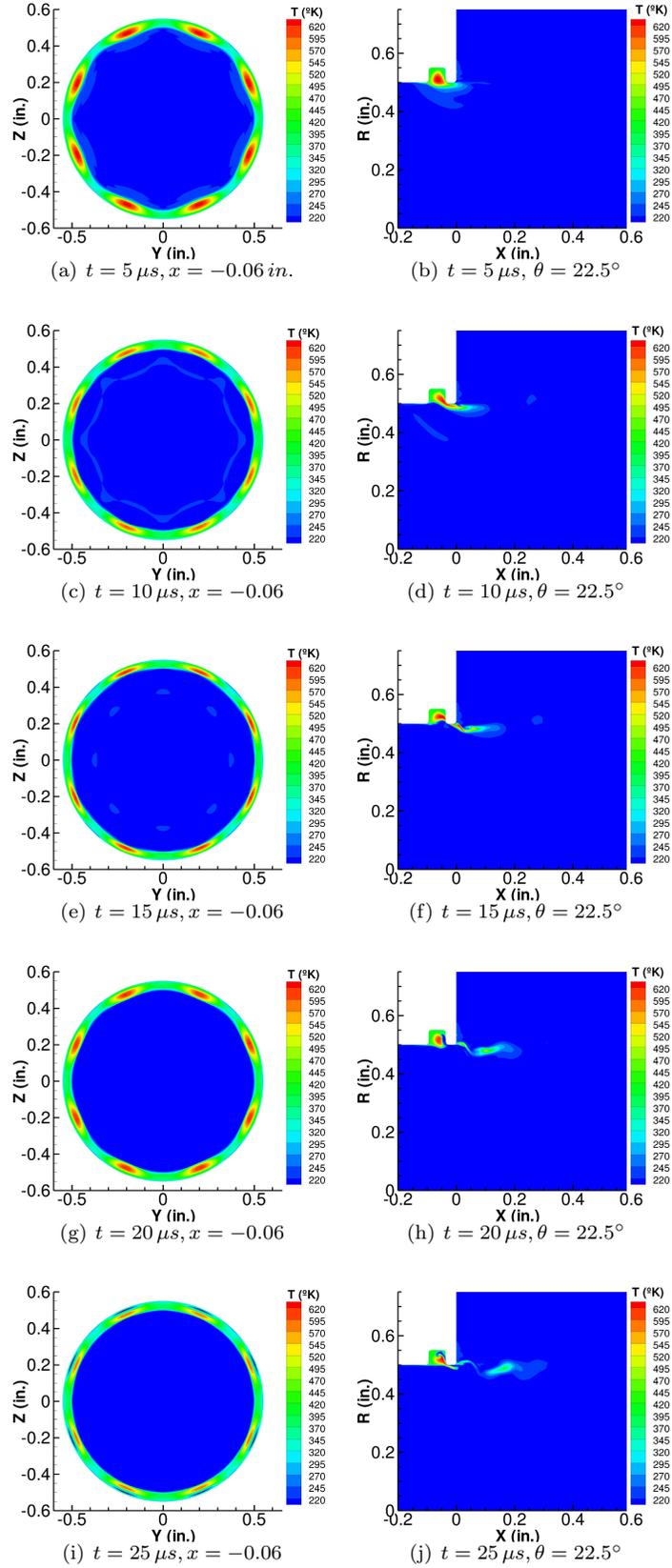
Figure 6. Temperature in a cross-stream and streamwise plane near the beginning of an actuator cycle.
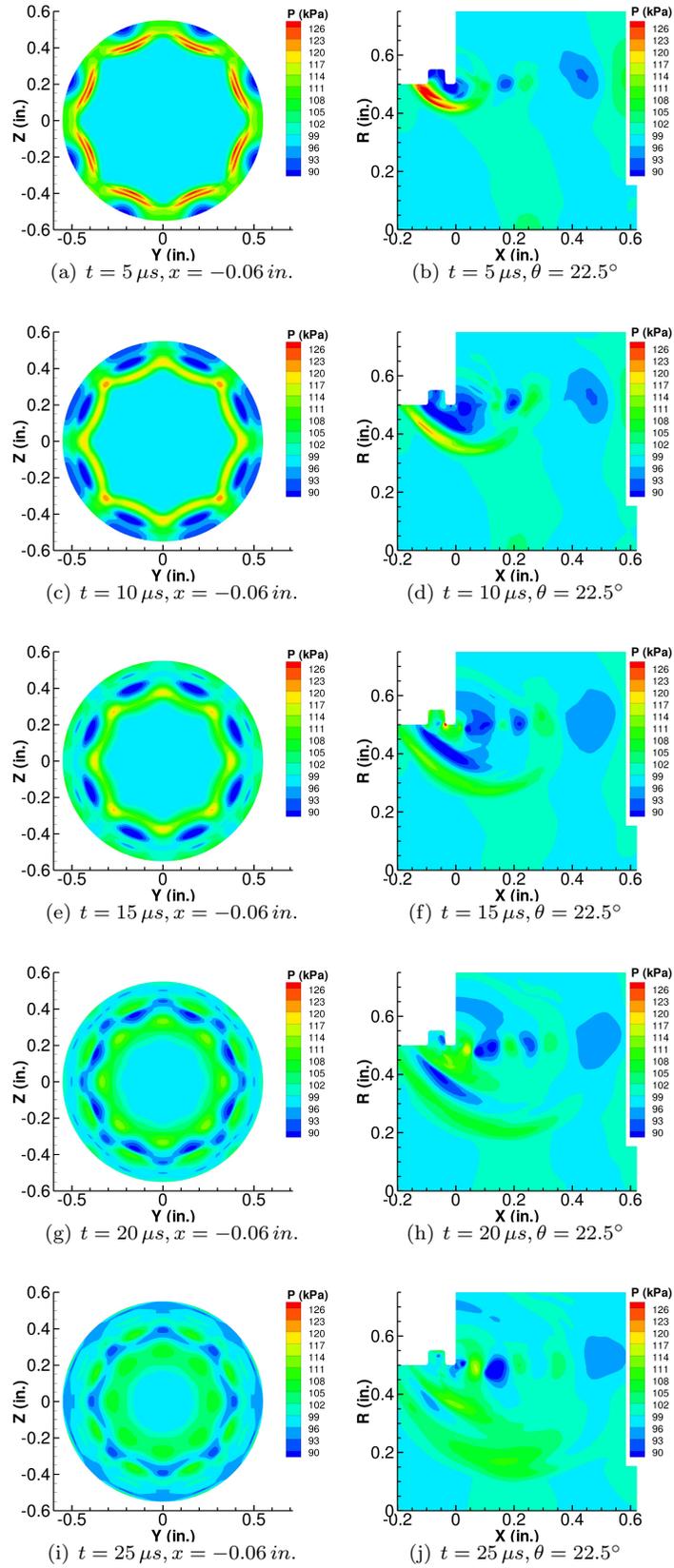
Figure 7. Pressure in a cross-stream and streamwise plane near the beginning of an actuator cycle.

be $1273°K$ ($1000°C$), based on emission spectroscopy measurements,[4] allowing the actuator energy to be calculated according to the procedure in Section II.A. Figure 4 shows the initial flow condition at the start of a cycle after the actuator energy has been added.

Experimental flow diagnostic data are difficult to acquire in the region near the actuator due to the close physical confines of the actuator cavity and nozzle exit as well as the electronic noise produced by the actuators. As a result, these simulations provide useful information into the actual forcing mechanisms behind the LAFPA that can not be acquired with experimental techniques. The lack of experimental data, however, also leaves few options for validating the performance of the actuator model. The LAFPA model, therefore, is evaluated against a theoretical understanding of the actuator physics and previous high fidelity simulation results.

The LAFPA model is based on the idea that rapid Joule heating creates a pressure wave that acts to perturb the jet. Figure 5 shows a series of instantaneous velocity vectors captured within the first $25\,\mu s$ of the start of an actuator cycle. The model operates on the internal energy so the velocity map at time $t = 0\mu s$ (figure 5(a)) is unchanged from the baseline (no actuator) flow. At $t = 5\mu s$ (figure 5(b)) the actuator energy has driven air out near the downstream corner of the actuator with a relatively high velocity. This rapid evacuation of air creates a void that begins filling from the upstream edge of the cavity at $t = 10\mu s$ (figure 5(c)). As the cavity refills, the high speed jet flow strikes the downstream corner of the actuator cavity and splits, pushing a second burst of fluid back into the jet and a new higher velocity pulse of air into the cavity ($t = 15\mu s$, figure 5(d)). This jet of fluid traveling upwards into the cavity restarts the flow recirculation at $t = 20\mu s$ (figure 5(e)) and $t = 25\mu s$ (figure 5(f)) as the flow near the actuator begins to return to its baseline state. The ejection of fluid from the cavity appears to be an important part of the actuator dynamics. Direct Numerical Simulations (DNS) of a LAFPA, using a model based on source terms in the flow equations and including a time component, have shown a similar behavior of fluid ejection.[5] However, the time component of the actuator added in the DNS simulations delayed slightly the time before the actuator began refilling with fluid due to the continued addition of energy to simulate the duty cycle. It has not yet been determined whether or not this delay is important to the downstream jet dynamics.

Simulations indicate that the LAFPA operates, at least in part, as a fluidic type actuator when air is forced from the actuator cavity as a result of the rapid addition of thermal energy. This thermal energy must be transported with the fluid or the temperature in the cavity will slowly increase. Figure 6 shows the instantaneous temperature, in a cross-stream and streamwise plane, during the first $25\,\mu s$ of a cycle. The peak temperature drops considerably from the initial $T_A = 1273°K$ over the first $5\,\mu s$ (figures 6(a) and 6(b)), the region of high temperature fluid remains concentrated in the cavity. Then, over the next $10\,\mu s$ (figures 6(c) - 6(f)), some of the hot gas is forced from the cavity. As jet flow begins to refill the cavity (figure 6(g) - 6(j)), the high temperature gas is trapped in the cavity as the flow recirculation in the cavity is restarted. This is consistent with the DNS simulation results of Kleinman et. al. that showed an area of high temperature fluid remaining in the recirculating cavity flow after an initial pulse of hot fluid was ejected.[5] A comparison of the cross-stream and streamwise views shows that the movement of high temperature gas goes downstream and into the initial shear layer of the jet rather than in the azimuthal direction around the jet. In fact, the only changes in the azimuthal temperature profile appear to be caused by the high temperature region moving axially in and out of the viewing plan. The contribution of the high temperature fluid (as opposed to a similar fluid at the jet exit temperature) to the perturbation of the jet is not yet fully understood.

The LAFPA appears to perturb the initial jet shear layer by forcing hot gas from the actuator and into the jet. Some experimental data, acquired using Schlieren imaging, indicates that rapid burst arc regime type plasma actuators generate a pressure wave that creates a perturbation by acting similar to a solid surface in the jet.[6,7] Figure 7 shows cross-stream and streamwise images of the instantaneous pressure during the first $25\,\mu s$ of the actuator cycle. At $t = 5\,\mu s$, a strong compression wave is visible in the streamwise view traveling upstream away from the actuator (figure 7(b)). In the cross-stream view, the high pressure waves leave the actuator cavity, traveling towards the jet centerline while spreading in the azimuthal direction. The pressure waves weaken as they travel and spread but leave a region of low pressure in their wake which appears to strongly influence the initial shear layer at $t = 10\,\mu s$ (figure 7(d)). When the cavity begins refilling at $t = 15\,\mu s$ (according to the velocity data in figure 5(d)), the high velocity flow creates a high pressure spot at the downstream corner of the actuator cavity where the flow stagnates (figure 7(f)). The pressure waves continue to spread and at $t = 25\,\mu s$ have penetrated to within $0.15\,in.$ of the jet centerline (figures 7(i) - 7(j)). By penetrating so far into the jet, it raises questions about whether the actuators impact only on the
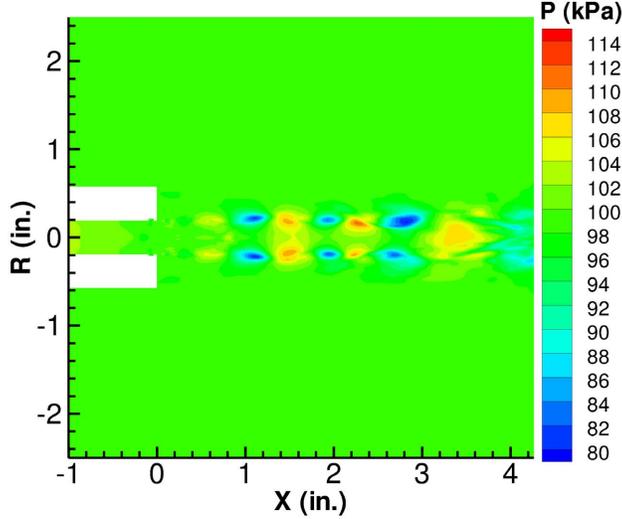
Figure 8. Instantaneous pressure at the end for the 4th actuator cycle taken from a slice through the middle of an actuator ($\theta = 22.5°$).

jet shear layer to excite the jet or if they also operate on the jet column itself. This will have implications on the scalability of the LAFPA system if the actuators must affect the jet column.

Experimental studies have demonstrated the ability of the LAFPA to excite a high speed high Reynolds number jet. Simulations incorporating the actuators in a jet indicate that their effect is induced by a rapid rise in temperature. This temperature change quickly expands the air in the cavity, generating a pressure wave that travels from the cavity and into the jet. It is this pressure wave that appears to actually perturb the jet (changing the pressure term in the momentum equation). A small amount of hot fluid is also ejected from the cavity but appears to only have a secondary role in any excitation. Data is now needed farther downstream in the jet plume to validate the actuator model and investigate to optimum excitation parameters for noise reduction.

III.B. Jet Dynamics

A jet is said to be excited when particular instabilities are amplified by an external force. These external perturbations may occur naturally (e.g. combustor tones) or specifically input at the nozzle exit for desired control. A simulation, using the LAFPA model described in section II.A, was run to excite the axisymmetric mode ($m = 0$) of a $M_j = 0.9$ isothermal jet near the preferred jet frequency at $St = 0.3$ ($4\,kHz$, $T = 0.00025\,s$). Figure 8 shows the instantaneous pressure in the jet after four complete actuator cycles. At this point in the simulation, the first actuator perturbation is approximately $x/D_j = 4$ downstream of the nozzle exit. The regularly spaced regions of high and low pressure show the location of the flow structures associated with the actuators. As seen in flow visualization experiments,[2] the paired flow structures on the top and bottom of the jet are characteristic of axisymmetric mode excitation. It appears, therefore, that the actuator perturbations are affecting the downstream jet dynamics in an expected manner.

The perturbations input by the flow actuators at the nozzle exit travel downstream where they are amplified by the jet. A simulation was run through four complete actuator cycles to acquire data in the first $x/D_j = 3.75$ downstream of the nozzle exit. The complete flow field was sampled every $5\mu s$ ($f = 200\,kHz$) during the fourth cycle for analysis. Figure 10 shows the fluctuations in pressure and temperature as a function of time and axial location. At $x/D_j = 0.5$ along the nozzle lipline ($r/D_j = 0.5$), a temperature increase precedes the pressure wave (figure 9(a). This supports analysis of the actuator dynamics which showed the high temperature fluid quickly leaving the actuator cavity and entering the initial shear layer. The levels, however, show that the temperature increase at this location is small relative to strength of the pressure wave.

The excited jet will amplify the pressure fluctuations input by the actuator the plume develops while the hot gas ejected from the cavity mixes with the surrounding jet flow and ambient air. Figure 9(b) shows

(a) $X = 0.5\,in.$

(b) RMS fluctuating quantities.
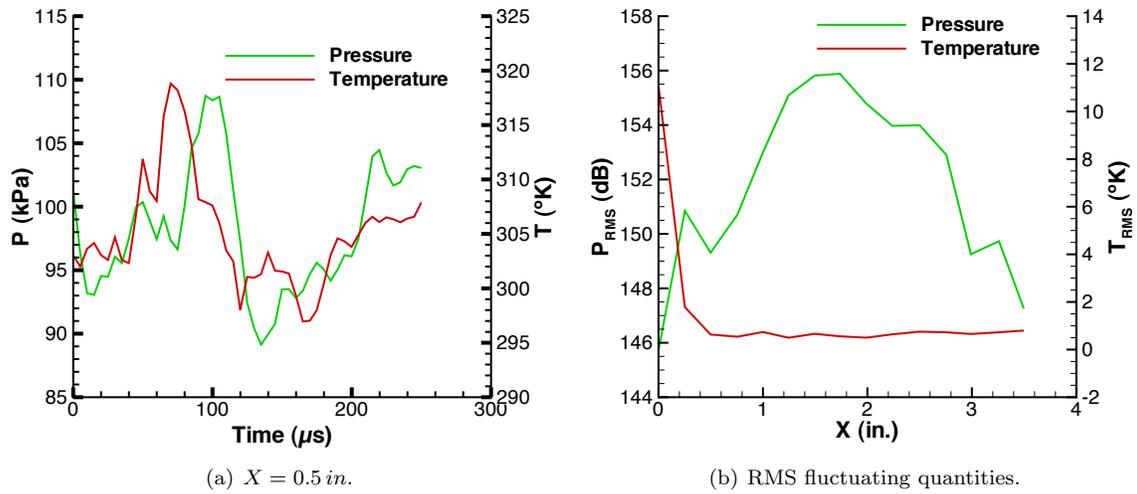
Figure 9. Pressure and temperature fluctuations along the nozzle lipline in the jet plume.

(a) Axial growth and decay of pressure fluctuations.

(b) Computational mesh near the nozzle exit with pressure contours.
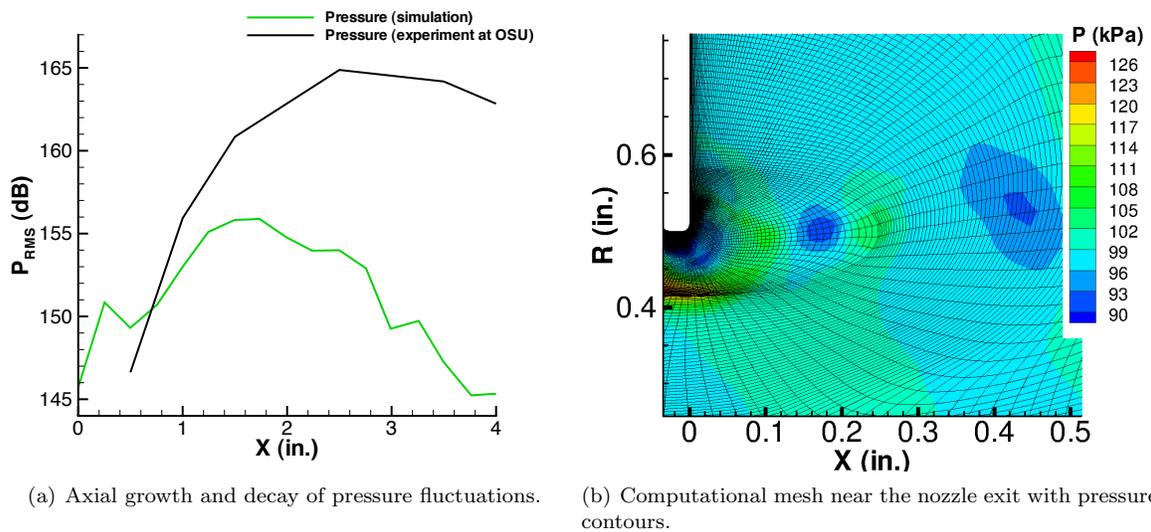
Figure 10. Pressure fluctuations along the nozzle lipline and in the initial jet plume.

an RMS average of the fluctuating temperature and pressure along the nozzle lipline as a function of axial location. The largest temperature fluctuations occur at the nozzle exit as expected but then the fluctuations quickly approach zero indicating that the high temperature fluid is rapidly dispersed. This supports the idea that temperature is a secondary force in the LAFPA perturbations. The axial development of the fluctuating pressure has an overall growth and decay pattern that indicates the jet is responding to the actuator inputs and the simulation is capturing this behavior to some extent. The data in figure 10(a), however, shows that the simulation results are differ significantly from experimental measurements.

Fluctuating pressure data acquired in experiments at OSU have documented the growth and decay of the actuators perturbations in the jet plume.[2] These experimental data show that the initial instability growth rate should be faster, growing approximately $20\,dB$ from $x/D_j = 0.5$ to $x/D_j = 2$, than the growth rate captured in the simulation (figure 10(a). Also, the experimental data show the peak, or saturation, point near $x/D_j = 3$, farther downstream than the peak at $x/D_j = 1.75$ determined in the simulation. This comparison shows that there are some serious limitations in the current simulations.

The growth and peak of perturbations in a jet is characterized by an initial growth rate (slope), given by linear stability theory, and a saturation or peak amplitude and location determined by non-linear effects. The perturbation computed in the simulation grows at a rate similar to the measured perturbation but only in the first $x/D_j = 0.25$ of the jet. The perturbation amplitude then abruptly decreases, from $x/D_j = 0.25$ to $x/D_j = 0.5$, before beginning to rise again. This behavior is not supported by theory. According to classic stability theory, the growth rate should be independent of the initial perturbation amplitude and, therefore, changes to the actuator power should not affect the growth rate beyond compensating for excess dissipation in the CFD simulation. Figure 10(b) shows the pressure contours in the near nozzle region with the computation mesh imposed. Because internal surfaces were required to hold grid points near corners at the actuator cavity and nozzle lip when the grid stretching is routine is applied, there is a elliptic boundary that points can not cross when the grid stretching is applied. As a result, there is a region where the grid is stretched more rapidly (from $x/D_j = 0.1$ to $x/D_j = 0.25$) than it should be. The seven-point DRP scheme employed in these simulations requires a minimum of 6 grid points across a flow structure to resolve the linear fluid dynamics (more points are required for non-linear behavior). The BASS code also aggressively dissipates unresolved flow structures to remove them from the solution and increase numerical stability. In figure 10(b), there are not enough grid points to resolve the flow structure centered near $x/D_j = 0.175$. As a result, the structure will be dissipated by the code. Downstream of this artificial boundary, the grid density increases allowing the portion of the flow structure not dissipated by the CFD filter to grow again. Note that the dissipation does not occur immediately so the results of the dissipation appear slightly downstream of the changes in the grid. So although the largest changes in the simulated flow appear slightly downstream of the stretched grid region, the limitations in the growth rate and saturation amplitude computed in the simulation are likely due issues with the computation grid. A grid sensitivity study, conducted using an entirely new grid topology, is needed to address these issues before the jet dynamics can accurately studied.

IV.   Conclusions

The Localized Arc Filament Plasma Actuators (LAFPA) have demonstrated the ability to excite a high-speed jet in experiments conducted at OSU. Simulations may offer a cost effective method to study the relationship between the LAFPA and the jet while optimizing the excitation for different applications. A model of the LAFPA for use in such simulations has been developed and applied in a three dimensional Large Eddy Simulation (LES) of an excited jet. The data collected from the simulation shows that the rapid heating introduced by the plasma actuators forces hot gas from the actuator cavity and initiates a pressure wave that alters the jet flow near the nozzle exit. Although the rapid heating starts the process, the data indicates that the high temperature of the gas only has a small role in the altering the downstream dynamics of the jet. Rather, it is the pressure wave that has the most dramatic effect on the jet and drives the excitation.

A total of four actuator cycles were simulated using the LAFPA model in the first attempt to accurately capture the unsteady dynamics of an excited jet using a LES simulation. The data collected shows an overall trend that qualitatively agrees with experimental measurements but does not sufficiently capture jet dynamics for scientific study. Analysis indicates that these deficiencies likely originate with the computational grid. A grid sensitivity study, therefore, is now required to improve future simulations.

Simulating the unsteady fluid dynamics in an excited jet is a difficult problem. The difficulties are enhanced when the LAFPA flow actuators, which operate on a very small time-scale and induce steep gradients in the flow, are included in the simulation. However, such simulations appear possible based on this first effort. The fluid dynamics near the actuator were studied and appear reasonable based on the information available. In the jet plume, the success of future simulations is dependent on the computational grid which must have enough grid density to resolve both linear and non-linear effects near the actuator and in the jet plume. This work is ongoing and the ability to perform this simulations will continue to develop. Ultimately, these excited jet simulations will be used to develop the LAFPA system for future large-scale application and to optimize the perturbation input for maximum effect.

References

[1] Brown, Clifford A., "Effect of Turbulence Modeling on an Excited Jet", AIAA 2009-3191, May 2009.

[2] Samimy, M., Kim, J.-H., Kastner, J., Adamovich, I., and Utkin, Y., "Active Control of a Mach 0.9 Jet for Noise Mitigation Using Plasma Actuators", AIAA J., Vol. 45(4), pp. 890-901, 2007.

[3] Samimy, M., Kastner, J., Kim, J.-H., Utkin, Y., Adamovich, I., and Brown, C., "Flow and Noise Control in High Speed and High Reynolds Number Jets Using Plasma Actuators", AIAA 2006-2846, June 2006.

[4] Utkin, Y., Keshav, S., Kim, J.-H., Kastner, J., Adamovich, I., and Samimy, M., "Development and Use of Localized Arc Filament Plasma Actuators for High-Speed Flow Control", J. of Physics D: Applied Physics, Vol. 40, pp. 685-694, 2007.

[5] Kleinman, R. R., Bodony, D. J., and Freund, J. B., "Numerical Modeling of Plasma Actuators in High Speed Jets", AIAA 2009-3190, May 2009.

[6] Leonov, S., Bityurin, V., Savelkin, K., and Yarantsev, D., "Effect of Electrical Discharge on Separation Processes and Shock Position in Supersonic Airflow", AIAA 2002-0355, January 2002.

[7] Leonov, S., Bityurin, V., and Yarantsev, D., "The Effect of Plasma Induced Separation", AIAA 2003-3853, 2003.

[8] Brown, Clifford A., "Scalability of the Localized Arc Filament Plasma Actuators", AIAA 2008-3043, May 2008.

[9] Hixon, R., Nallasamy, M., and Sawyer, S., "Parallelization Strategy for an Explicit Computational Aeroacoustics Code", AIAA 2002-2583, July 2002.

[10] Hixon, R., Nallasamy, M., Sawyer, S., and Dyson, R., "Comparison of Numerical Schemes for a Realistic Computation Aeroacoustics Problem", International Journal of Aeroacoustics, Vol. 3, pp. 379-397, 2004.

[11] Hixon, R., Bhate, D., Nallasamy, M., and Sawyer, S., "Shock-Capturing Dissipation Schemes for High-Accuracy Computational Aeroacoustics (CAA) Codes", AIAA 2006-2413, May 2006.

[12] Hixon, R., Nallasamy, M., and Sawyer, S., "Progress towards the prediction of turbomachinery noise using Computational Aeroacoustics", Inter-Noise IN06-116, Dec. 2006.

[13] Nallasamy, M., Hixon, R., and Sawyer, S., "Solution of unsteady Euler equations: Gust-cascade interaction tones", Computers and Fluids, Vol. 36, pp. 724-741, 2007.

[14] Grinstein, F., Drikakis, D., Fureby, C., and Youngs, D., "Transistion and Turbulence Decay in the Taylor-Green Vortex", AIAA 2006-0698, Jan. 2006.

[15] Hixon, R., Allampali, V., Nallasamy, M., and Sawyer, S., "High-Accuracy Large-Step Explicit Runge-Kutta (HALE-RK) Schemes for Computational Aeroacoustics", AIAA 2006-0797, Jan. 2006.

[16] Tam, C. K. W. and Webb, J. C., "Dispersion-relation-preserving finite-difference schemes for computational acoustics", J. of Computational Physics, Vol. 107, pp. 262-281, 1993.

[17] Thompson, K. W., "Time dependent boundary conditions for hyperbolic systems", J. of Computational Physics, Vol. 68, pp. 1-24, 1987.

[18] Thompson, K. W., "Time dependent boundary conditions for hyperbolic systems II", J. of Computational Physics, Vol. 89, pp. 439-461.

[19] Goodrich, J., "A Comparison of Three PML Treatments for CAA (and CFD)", AIAA 2008-2922, May 2009.

[20] Hixon, R. and Allampalli, V., "Optimization of Finite-Difference Boundary Stencils for Improved Viscous Stablility", AIAA 2010-837, Jan. 2010.

[21] Hixon, R., "On Increasing the Accuracy of MacCormack Schemes for Aeroacoustics Applications", AIAA 1997-1586, 1997.

[22] GridPro/az3000, Program Development Corporation, White Plains, NY.

REPORT DOCUMENTATION PAGE

1. REPORT DATE (DD-MM-YYYY) 01-04-2011	2. REPORT TYPE Technical Memorandum	3. DATES COVERED (From - To)

4. TITLE AND SUBTITLE
LES of a Jet Excited by the Localized Arc Filament Plasma Actuators

5a. CONTRACT NUMBER

5b. GRANT NUMBER

5c. PROGRAM ELEMENT NUMBER

6. AUTHOR(S)
Brown, Clifford, A.

5d. PROJECT NUMBER

5e. TASK NUMBER

5f. WORK UNIT NUMBER
WBS 984754.02.07.03.17.03

7. PERFORMING ORGANIZATION NAME(S) AND ADDRESS(ES)
National Aeronautics and Space Administration
John H. Glenn Research Center at Lewis Field
Cleveland, Ohio 44135-3191

8. PERFORMING ORGANIZATION REPORT NUMBER
E-17625

9. SPONSORING/MONITORING AGENCY NAME(S) AND ADDRESS(ES)
National Aeronautics and Space Administration
Washington, DC 20546-0001

10. SPONSORING/MONITOR'S ACRONYM(S)
NASA

11. SPONSORING/MONITORING REPORT NUMBER
NASA/TM-2011-216984

12. DISTRIBUTION/AVAILABILITY STATEMENT
Unclassified-Unlimited
Subject Category: 71
Available electronically at http://www.sti.nasa.gov
This publication is available from the NASA Center for AeroSpace Information, 443-757-5802

13. SUPPLEMENTARY NOTES

14. ABSTRACT
The fluid dynamics of a high-speed jet are governed by the instability waves that form in the free-shear boundary layer of the jet. Jet excitation manipulates the growth and saturation of particular instability waves to control the unsteady flow structures that characterize the energy cascade in the jet. The results may include jet noise mitigation or a reduction in the infrared signature of the jet. The Localized Arc Filament Plasma Actuators (LAFPA) have demonstrated the ability to excite a high-speed jets in laboratory experiments. Extending and optimizing this excitation technology, however, is a complex process that will require many tests and trials. Computational simulations can play an important role in understanding and optimizing this actuator technology for real-world applications. Previous research has focused on developing a suitable actuator model and coupling it with the appropriate computational fluid dynamics (CFD) methods using two-dimensional spatial flow approximations. This work is now extended to three-dimensions (3-D) in space. The actuator model is adapted to a series of discrete actuators and a 3-D LES simulation of an excited jet is run. The results are used to study the fluid dynamics near the actuator and in the jet plume.

15. SUBJECT TERMS
Aerodynamic noise

16. SECURITY CLASSIFICATION OF:

a. REPORT	b. ABSTRACT	c. THIS PAGE	17. LIMITATION OF ABSTRACT	18. NUMBER OF PAGES	19a. NAME OF RESPONSIBLE PERSON STI Help Desk (email:help@sti.nasa.gov)
U	U	U	UU	21	19b. TELEPHONE NUMBER (include area code) 443-757-5802